Adeno-associated viral vector-mediated gene transfer results in long-term enzymatic and functional correction in multiple organs of Fabry mice

Sung-Chul Jung*, Ina P. Han*, Advait Limaye*, Ruian Xu†, Monique P. Gelderman*, Patricia Zerfas‡, Kamala Tirumalai§, Gary J. Murray*, Matthew J. During†¶, Roscoe O. Brady*, and Pankaj Qasba*‖

*Developmental and Metabolic Neurology Branch, ‡Electron Microscopy Facility, National Institute of Neurological Disorders and Stroke, §Laboratory of Cellular and Molecular Immunology, National Institute of Allergy and Infectious Diseases, National Institutes of Health, Bethesda, MD 20892; †Department of Molecular Medicine, University of Auckland School of Medicine, 85 Park Road, Auckland, New Zealand; and ¶Department of Neurosurgery, Thomas Jefferson University, Philadelphia, PA 19107

Contributed by Roscoe O. Brady, December 29, 2000

Fabry disease is a lysosomal storage disorder caused by a deficiency of the lysosomal enzyme α-galactosidase A (α-gal A). This enzyme deficiency leads to impaired catabolism of α-galactosyl-terminal lipids such as globotriaosylceramide (Gb3). Patients develop painful neuropathy and vascular occlusions that progressively lead to cardiovascular, cerebrovascular, and renal dysfunction and early death. Although enzyme replacement therapy and bone marrow transplantation have shown promise in the murine analog of Fabry disease, gene therapy holds a strong potential for treating this disease in humans. Delivery of the normal α-gal A gene (cDNA) into a depot organ such as liver may be sufficient to elicit corrective circulating levels of the deficient enzyme. To investigate this possibility, a recombinant adeno-associated viral vector encoding human α-gal A (rAAV-AGA) was constructed and injected into the hepatic portal vein of Fabry mice. Two weeks postinjection, α-gal A activity in the livers of rAAV-AGA-injected Fabry mice was 20–35% of that of the normal mice. The transduced animals continued to show higher α-gal A levels in liver and other tissues compared with the untouched Fabry controls as long as 6 months after treatment. In parallel to the elevated enzyme levels, we see significant reductions in Gb3 levels to near normal at 2 and 5 weeks posttreatment. The lower Gb3 levels continued in liver, spleen, and heart, up to 25 weeks with no significant immune response to the virus or α-gal A. Also, no signs of liver toxicity occurred after the rAAV-AGA administration. These findings suggest that an AAV-mediated gene transfer may be useful for the treatment of Fabry disease and possibly other metabolic disorders.

Fabry disease is an X-linked inborn error of glycolipid metabolism caused by deficiency of the lysosomal enzyme α-galactosidase A (α-gal A; EC 3.2.1.22) (1). The enzyme is responsible for hydrolysis of the terminal α-galactoside linkage in various glycolipids. The deficiency results in the body's inability to break down globotriaosylceramide (Gb3), also known as ceramide trihexoside. The glycolipid accumulates predominantly in the endothelial lining of blood vessels within the kidney, heart, liver, spleen, and in the plasma of the patients. With increasing age a progressive accumulation of the glycolipid occurs in vital organs, resulting in renal, cardiac, and cerebrovascular complications in the Fabry patients. The genomic sequences and cDNAs encoding both human and mouse α-gal A have been isolated (2–4). A mouse model of Fabry disease has been generated by targeted disruption of the α-gal A gene (5). These α-gal A-deficient mice appear clinically normal but display accumulation of Gb3 in several organs, similar to that observed in Fabry patients. In the Fabry mice, a substantial accumulation of Gb3 is seen between 3 and 6 months and the glycolipid load continues to accumulate progressively throughout the lifespan of the animal. This similarity in metabolite accumulation between Fabry mice and human Fabry patients

makes this model useful for evaluation of various therapeutic strategies.

A portion of the hydrolytic enzymes implicated in lysosomal storage disorders is secreted rather than trafficked directly to lysosomes (6, 7). However these secreted enzymes can be recaptured via the mannose-6-phosphate receptors by adjacent and distant cells, a phenomenon commonly referred as receptor-mediated endocytosis (6–9). Although, other receptor-mediated pathways also may be involved, this mechanism for secretion and recapture of α-gal A by gene-corrected cells could prove advantageous to therapy for lysosomal storage disorders by lessening the proportion of target cells that must be corrected to obtain a clinical benefit.

The premise of secretion and recapture of the lysosomal enzyme provides a strong rationale for the use of somatic or enzyme replacement methods. However, the use of enzyme therapy (10) presents limitations of short half-life, frequent administration, host immune response, and requirement of large quantities of the enzyme. Other corrective methods including recombinant retrovirus (11–13), bone marrow transplantation (14), and recombinant adenovirus (15) also present severe restrictions. Adenoviral gene transfer vectors generate severe immune responses despite their high efficiency. Retroviral vector gene transfer and plasmid transfer cannot be used for the treatment of Fabry disease due to low efficiency.

To address some of these limitations, we evaluated the use of adeno-associated virus (AAV) that has been extensively used as a potential gene delivery vehicle (16, 17). AAV is a single-stranded DNA virus that is nonpathogenic, can transduce both dividing and nondividing cells, and achieve long-term expression of therapeutic genes with no apparent adverse effects. In this study we describe a successful AAV-mediated gene delivery of α-gal A, using the human EF1-α promoter. The virus containing EF1-α-AGA transgene delivered directly to the liver via the hepatic portal vein resulted in a long-term correction of both the enzyme and the glycolipid storage defect in the Fabry mouse model.

Materials and Methods

Construction of rAAV-AGA Viral Vector. The parent AAV plasmid pAM/EF-pL-WPRE-BGHpoly(A) was created as described (18) with minor modifications. Full-length human α-gal A cDNA

---

was subcloned into pAM/EF-pL-WPRE-BGHpoly(A). The rAAV-AGA virus was generated by using a helper free packaging system (19). Both pAM/EF-hAGA-WPRE-BGHpoly(A) and pAd/AAV (which contains both the *rep* and *capsid* open frames of AAV flanked by adenovirus terminal repeats, but lacks the inverted terminal repeats of AAV) were transfected into 293 cells using calcium phosphate. At 24 h after transfection, the 293 cells were infected with adenovirus dl309 at a multiplicity of infection (moi) of 5. At 48 h after infection, the viruses were harvested by using sonication. The crude extract was heat-inactivated and then purified by using ammonium sulfate followed by cesium chloride density gradient centrifugation and dialyzed against PBS and further concentrated. All vector stocks were assayed for adenovirus contamination using a plaque assay on permissive 293 cells and were completely free of adenovirus. The rAAV-AGA viral vector titer was determined by quantitative PCR using ABI 7700 (Perkin–Elmer/Applied Biosystems).

Cell Lines. Human 293 cells (20) grown in Iscove's modified Eagle's medium supplemented with 10% FBS were used. The human fibroblast cells from patients with Fabry disease were grown in medium 199 with added L-glutamine (4 μM/ml) and 10% FBS.

Animals. All animals used in this study were maintained in the C57BL/6 $\times$ 129/svJ hybrid background. Mice were housed in a National Institutes of Health mouse facility accredited by the American Association for the Accreditation of Laboratory Animal Care and were fed autoclaved diet and water. Mice were between the ages of 10 and 12 weeks at the inception of the study. All mice were genotyped by PCR as described (5). Mice were anesthetized with ketamine/xylazine and injected with 1×10^{11}–1×10^{13} viral particles of rAAV-AGA via the hepatic portal vein. Animals were killed and analyzed at 2, 5, 15, and 25 weeks after rAAV-AGA administration. The liver, spleen, kidneys, heart, small intestines, and lungs were harvested from each rAAV-injected Fabry mouse along with age-matched wild-type control mice and untreated Fabry mice for analysis. Blood samples were collected from the tail vein at various time points. Aspartate transaminase, alanine transaminase, and other enzymes were measured by the clinical pathology department at the National Institutes of Health.

α-Gal A Assay and Western Blot. Fluorimetric assay of α-gal A was performed as described (21) with minor modifications. Tissue samples were homogenized and sonicated in an aqueous buffer (28 mM citric acid/44 mM disodium phosphate/5 mg/ml sodium taurocholate, pH 4.4) and then centrifuged at $20,000 \times g$ for 30 min. α-Gal A activity was determined by incubating aliquots of the supernatant solution at 37°C with 5 mM 4-methylumbelliferyl-α-D-galactopyranoside in the same buffer without taurocholate and with added BSA (4 mg/ml) in the presence of 0.1 M N-acetylgalactosamine, a specific inhibitor of N-acetylgalactosaminidase. Western blots were performed as described (22).

Quantitation of Gb3 Levels. Lipids were extracted (23) and saponified, and a glycolipid fraction was obtained essentially as described (24). The glycolipid fraction was dissolved in a minimum volume of chloroform/methanol (2:1) and chromatographed on a Luca 3 Silica column (150×4.6 mm) from Phenomenex, Torrance, CA. Glycolipids were eluted with a solvent composed of chloroform/methanol/water/ammonia (66:30:3.5:0.5) and determined quantitatively by using a Sedex 55 evaporative light scattering detector (ESLD). The evaporator on the ESLD was set at a temperature of 50°C, nitrogen pressure was 2.4 bar and the gain was at 10. Standard Gb3 was obtained from Matreya, Pleasant Gap, PA.

Immunofluorescent Staining of Gb3. Immunofluorescent staining of Gb3 was performed according to the method described (25) with some modifications. Cells grown on cover slips or frozen-sectioned tissues were fixed with 4% paraformaldehyde in PBS for 30 min at 4°C. After removal of fixing solution, the specimens were rinsed in PBS and blocked with 5% BSA in PBS for 1 h at room temperature. The specimens were then incubated with monoclonal mouse anti-Gb3 IgG (kindly supplied by H. Sakuraba, The Tokyo Metropolitan Institute of Medical Science, Tokyo) at 4°C overnight, followed by washing with ice-cold PBS. Specific binding was visualized with fluorescein isothiocyanate-conjugated F(ab')$_2$ goat anti-mouse IgG with a confocal laser microscope (Leica, Deerfield, IL).

Electron Microscopy. Tissues were immersion fixed in 2% glutaraldehyde and 2% formaldehyde in 0.1 M sodium cacodylate buffer at pH 7.4. The tissue blocks then were fixed in 0.2–1% OsO$_4$ in 0.1 M cacodylate buffer for 1 h, washed, and postfixed with 0.5% uranyl acetate in 50% ethanol for 1 h, serially dehydrated in ethanol and propylene oxide, and embedded in epoxy resin. Thin sections were counterstained with uranyl acetate and lead citrate.

Anti-α-Gal A Immune Response. Sera were collected at designated time points, and antibody responses against α-gal A were measured by ELISA as described (26) with some modifications. Briefly, 96-well, flat-bottom microtiter plates were coated with α-gal A (1 μg/ml) in PBS-sodium azide buffer and incubated overnight at 4°C. After washing in 0.05% Tween-PBS, plates were blocked in 10% casein-PBS for 1 h at 37°C. Subsequently, sera were serially diluted in antibody buffer (0.5% BSA-PBS, pH 8.0) and incubated for 1 h at 37°C. After washing, alkaline phosphatase-conjugated goat anti-mouse IgG was added in a volume of 50 μl per well and incubated for 1 h at 37°C. Individual IgG isotypes were detected by using either alkaline phosphate-conjugated rat anti-mouse IgG1, or rat anti-mouse IgG2a (ICN). Substrate (Kirkegaard & Perry Laboratories) was added (100 μl/well) and incubated for 30 min. The optical density at 635 nm was determined with a Versamax Microplate reader (Molecular Devices). The endpoint dilutions were defined as the serum dilution at which the absorbance at 635 nm equaled 2.5 times the absorbance of preimmune serum.

Results

rAAV-AGA Expression and Activity *in Vitro*. Fabry patient fibroblast cells were transduced to test the effectiveness of the rAAV-AGA *in vitro*, before delivering the gene to an α-gal A-deficient mouse. The cDNA for the α-gal A gene is driven by a human EF1-α promoter and flanked by the regulatory element WPRE, and the polyadenylation site is provided by the BGHpoly(A). Fibroblasts infected at an moi of 1,000, at 50–60% cell density, consistently showed AGA expression 30% above the background (uninfected). This AGA expression level was sufficient to clear the glycolipid storage in the lysosomes of the transduced patient cells within 72 h of the infection. Fig. 1 shows the immunofluorescence staining of Gb3 in Fabry fibroblasts cells not transduced with rAAV-AGA. The accumulated Gb3 appears to be more pronounced within the lysosomal bodies in the cytoplasm whereas no lysosomal bodies are seen in the rAAV-AGA-transduced Fabry cells (Fig. 1 *a* and *c*). The Gb3 accumulation was analyzed by using a laser scanning confocal imaging system. Some background staining in these cells persist at lower moi, although, infection with higher moi (5,000) showed a more complete clearance of Gb3 as seen in Fig. 1*d*. It has been shown in previous reports that 5–10% enzyme level of the wild type was sufficient to clear the Gb3 from the cells (27, 28). Expression *in vitro* appears proportional (although not linear) with moi. The 293 human embryonic kidney cells appear to be more permissive
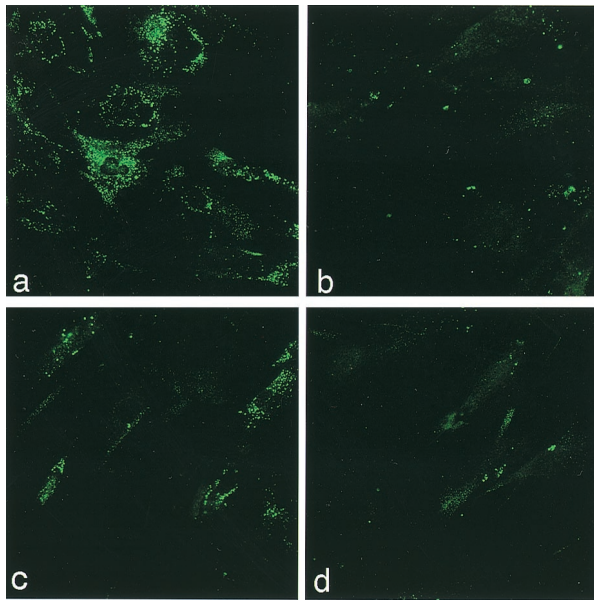
Fig. 2. Western blot analysis of α-gal A proteins in livers of Fabry mice at 2 weeks after rAAV-AGA infusion via hepatic portal vein. Lane 1, liver of untreated Fabry mouse. Lanes 2–5, livers of rAAV-AGA-treated Fabry mice. Lane 6, liver of wild-type mouse. Molecular mass of human α-gal A protein produced from rAAV-AGA vector should be 46 kDa. Molecular mass of mouse α-gal A protein from wild-type mouse is 50 kDa.

Fig. 1. FITC-labeled Gb3 staining of fibroblasts from Fabry patient and normal human fibroblasts. (*a*) Nontransduced Fabry fibroblasts and (*b*) normal fibroblasts. (*c*) Fabry fibroblasts transduced with rAAV-AGA at moi 1,000. (*d*) Fabry fibroblasts transduced with rAAV-AGA at moi 5,000.

and showed higher AGA expression levels at one-tenth the moi used for the human fibroblasts. We confirmed the specificity of the expressed AGA message and the enzyme in these and the patient cells with reverse transcriptase–PCR and Western blot analysis. The *in vitro* results confirmed that the rAAV-AGA vector was capable of delivering a functional transgene to the cells and successfully relieving the Gb3 load in patient fibroblast cells.

***In Vivo* Expression of α-Gal A after Hepatic Portal Vein Delivery of the Virus.** To demonstrate a similar metabolic correction in the α-gal A-deficient mice, a single injection of the rAAV-AGA was delivered via the hepatic portal vein. Approximately 1×10^{13} particles of the recombinant AAV-AGA were delivered to each Fabry mouse. Groups of the injected animals were euthanized at 2, 5, 15, and 25 weeks after treatment. Age-matched noninjected Fabry mice and their non-Fabry (wild type) littermates were also euthanized at similar time points. Initially expression of human α-gal A protein was tested in liver tissues by Western blot analysis. At 2 weeks, a robust signal against a polyclonal anti-human AGA is seen. Fabry mice that did not get the transgene showed no signal. The mouse AGA migrates slower on an SDS gel, indicating a slightly larger protein compared with the human recombinant AGA (Fig. 2). Enzyme activity in various tissues of the transduced animals is shown in Table 1. The AGA activities shown represent an average of the pooled results from each of the treated, untreated, and wild-type groups at different time points. Significantly higher enzyme levels (10- to 16-fold) are seen in the animals injected at 2 weeks compared with the untreated Fabry controls. In particular the liver and heart of the transduced animals show the largest increase over the enzyme levels of the untreated Fabry animals (Fig. 3). The AGA levels in liver are 28.5 ± 6% of enzyme activity of wild-type control mice. Similarly, heart shows an 18–20% relative increase in the AGA levels. In liver, the α-gal A enzyme activities at 5 and 15 weeks decline to 10.3 ± 1.4% and 5.5 ± 1.0%, respectively of age-matched, wild-type enzyme activities. It is not clear why the enzyme levels at 25 weeks show small increases in α-gal activity compared with 15 weeks. It appears that posttransduction, all
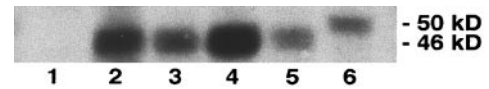
tissues show an increase in their relative AGA levels and more importantly, the enzyme increases persist for 6 months, demonstrating long-term expression of the recombinant human AGA.

Reduction of Gb3 in Different Organs. Treated Fabry mice were evaluated for Gb3 correction, using HPLC analysis. Liver by far showed the most impressive correction at 2, 5, 15, and 25 weeks at 92%, 97%, 55% and 76% respectively, compared with age-matched Fabry mice that did not get the treatment (Fig. 4). In addition to liver, spleen, heart, and lungs show minimal residual Gb3 and maximum correction at 2 and 5 weeks (Table 2). These results are consistent with previous reports that a single delivery of rAAV-gene(s) usually shows peak activity between 5 and 7 weeks (29, 30). Spleen, heart, and lungs show a relative clearance of 81%, 66%, and 77% respectively. With the exception of kidney, we also saw continued clearance at 15 and 25 weeks. We saw a reaccumulation in the Gb3 levels, in all tissues at 15 weeks posttreatment. However, these levels are still lower than the age-matched untreated Fabry mice. In contrast, we see evidence of continued Gb3 clearance in liver, spleen, and heart at 25 weeks. Both liver and heart showed a consistent lower Gb3 load at 6 months post-rAAV-AGA delivery. Electron microscopy analysis of the liver further indicates the effectiveness of a single rAAV-AGA injection in the mouse liver (hepatic portal vein). Livers from these mice showed significantly fewer inclusions in Kupffer cells and hepatocytes than in the livers from the untouched mice (Fig. 5). Similarly, using monoclonal anti-Gb3 antibody, little or no evidence of Gb3 accumulation is seen in the hepatocytes of the treated livers at 15 weeks posttreatment (Fig. 6). Typically, such staining in a Fabry tissue section would show lysosomal inclusions within the cytoplasm of the liver cell. Fig. 6*c* shows clearance of accumulated Gb3 not seen in the untreated Fabry mouse.

Examination of Potential Immune Response and Liver Toxicity. Sera were collected at various time points and analyzed for anti-AGA antibody by using ELISA. Of the rAAV-AGA transduced animals, 30–40% showed low titers of anti-AGA antibody. Although a full spectrum of isotypes was measured, the low titers belonged to a single subclass, IgG1. More importantly, the effect of these titers was without a consistent neutralizing response (data not shown). All of the control sera were negative for AGA-specific antibody at all time points. To rule out any liver damage or toxicity due to the direct delivery of rAAV-AGA infusion, various liver enzymes were tested. We found no difference in plasma aspartate transaminase or plasma alanine transaminase, marker enzymes for hepatic damage. The enzymes were monitored up to 14 days postinfection, using the predelivery levels as our base line. Levels of normal and rAAV-AGA-treated mice were 15 ± 0.7–17 ± 2.8 units/liter; 9 ± 1.5–15 ± 2.6 units/liter for alanine transaminase and 24 ± 0.7–29 ± 5.7 units/liter; 22 ± 0.6–32 ± 1.2 units/liter for aspartate transaminase, respectively. Also, the preinfection and postinfection total bilirubin levels were within the normal range (0.1 mg/dl). Histological examination of the infected liver sections by light

Table 1. α-Gal A enzyme activities in organs derived from mice killed at 2, 5, 15, and 25 weeks after rAAV-AGA treatment

Group (no. of mice)	Enzyme activity (nmole/hr per mg protein)					
	Liver	Spleen	Heart	Lung	Kidney	Small intestine
Wild-type mice (8)	72.5 ± 6.20	236.2 ± 26.90	7.2 ± 1.10	71.3 ± 14.80	32.5 ± 9.00	195 ± 40.40
Untreated Fabry mice (8)	1.4 ± 0.12	3.8 ± 0.94	0.3 ± 0.12	1.8 ± 0.26	1.2 ± 0.47	3.3 ± 1.55
Treated mice (4) 2 weeks postinjection	20.9 ± 4.53[†]	6.3 ± 4.36	1.4 ± 0.18[†]	3.9 ± 0.95	4.0 ± 4.65	22.3 ± 3.06[†]
Treated mice (4) 5 weeks postinjection	8.2 ± 1.14[†]	26.3 ± 0.03[†]	1.5 ± 0.21[†]	6.6 ± 0.40[†]	6.2 ± 0.08*	11.4 ± 3.25*
Treated mice (4) 15 weeks postinjection	3.8 ± 0.68[†]	18.0 ± 0.01[†]	0.6 ± 0.25	5.6 ± 1.63*	2.0 ± 0.01*	8.2 ± 2.20*
Treated mice (3) 25 weeks postinjection	6.0 ± 0.79[†]	30.3 ± 0.03*	1.3 ± 0.61	6.7 ± 1.02*	4.0 ± 0.03*	13.0 ± 5.00

*, $P < 0.05$ vs. untreated Fabry mice (unpaired t test); †, $P < 0.01$.

and electron microscopy also revealed no detectable damage (see Figs. 5 *c* and *d* and 6 *c* and *d*).

Discussion

Genetic modification of an appropriate depot organ such as liver appears attractive for the delivery of recombinant enzyme in the systemic circulation for disorders such as Fabry disease. This assumption is based on the fact that about 10% of the total Gb3 in the body is deposited in the liver (31, 32). In addition, the three-target cell types in liver play a central role in the Gb3 synthesis and turnover (33). The observations presented in this report and the data published by other investigators (34–36) add merit to the use of such a gene delivery for a variety of lysosomal storage disorders. In particular, the approach is attractive for Fabry disease, because: (*i*) Only a small proportion (5–10%) of

the normal enzyme activity is sufficient to restore therapeutic correction. It is known that Fabry heterozygotes can lead a normal life with only 10% of the normal enzyme activity (15). (*ii*) A proportion of the normally secreted lysosomal hydrolases get recaptured from the systemic circulation by adjacent and distant cells via the mannose-6-phoshate receptors (9). And more recently, Schiffman *et al.* (10, 37) have shown that AGA enzyme replacement results in reduced Gb3 storage and clinical improvement in Fabry patients. Applications of such a gene delivery also have been considered in the treatment of inborn errors of metabolism and the diseases where liver serves as a site for the secretion of the therapeutic proteins, factor IX for hemophilia B (38), and insulin analogue for diabetes (39).

Based on rationales presented, we examined the feasibility of a rAAV-AGA to correct the glycolipid storage defect in the murine model of Fabry disease. The availability of the Fabry mouse model has resulted in the use of several approaches currently being evaluated, including enzyme and gene replacement (10, 13) and glycosylation inhibitor (40). In this study we show that a single delivery of the rAAV-AGA to the Fabry mouse liver was sufficient to restore α-gal A activity to levels necessary to correct Gb3 levels. With the exception of kidney, this correction was seen in all of the visceral organs tested. More importantly, the glycolipid storage levels stayed at near normal levels for up to 5 weeks and persisted at levels 40–60% lower than the untreated Fabry animals up to 6 months.

The enzyme activity levels in the liver seem to peak 2 weeks postinfusion at 28.5 ± 6.2% of the normal enzyme activity. The AGA levels in spleen, heart, small intestine, and lung also showed modest increases. With the exception of liver (the delivery organ) and the heart, all other tissues show a delay in
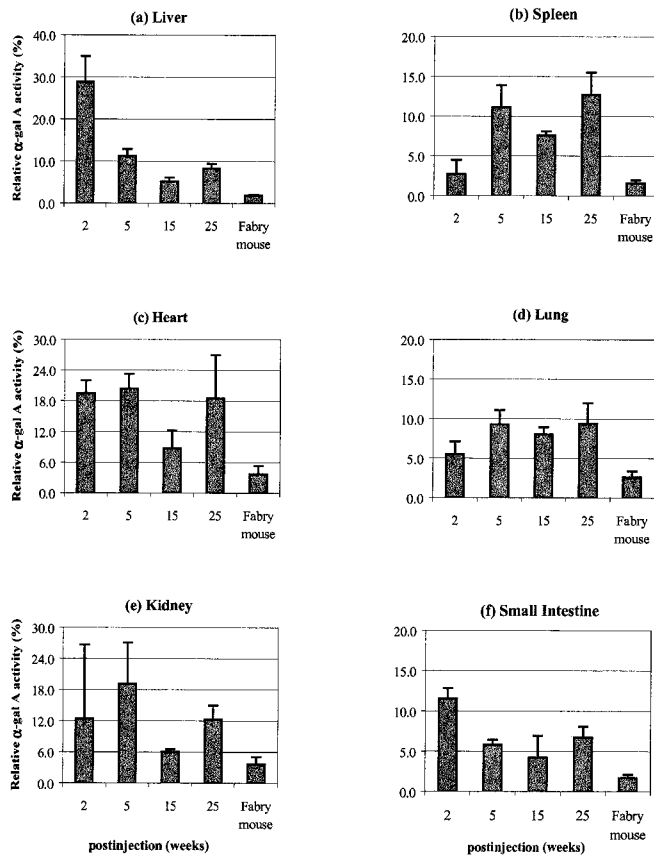

Fig. 3. Levels of α-gal A enzyme activities in tissues of Fabry mice after rAAV-AGA treatment. The levels of α-gal A activities (%) were expressed as a percentage of the levels found in age-matched wild-type mice. Values are presented as the mean ± SD.
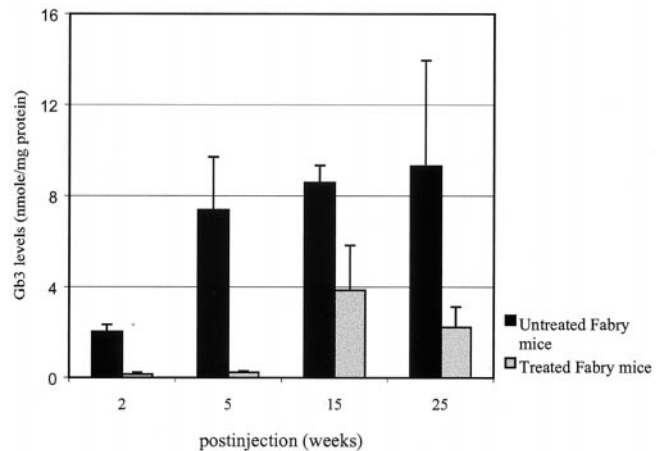

Fig. 4. Gb3 levels in livers of Fabry mice after rAAV-AGA treatment at 2, 5, 15, and 25 weeks and in age-matched untreated Fabry mice. Values are presented as the mean ± SD.

Jung et al.

Table 2. Gb3 levels in tissues from mice rAAV-AGA-injected mice killed at 2, 5, 15, and 25 weeks posttreatment

Tissue	Animals	Gb3 levels, nmole/mg protein			
		2 weeks	5 weeks	15 weeks	25 weeks
Liver	Untreated Fabry mice	2.02 ± 0.31	7.37 ± 2.34	8.58 ± 0.75	9.31 ± 4.64
	Wild-type mice	0.04 ± 0.01	0.05 ± 0.01	0.12 ± 0.01	0.05 ± 0.01
	Treated Fabry mice	0.15 ± 0.09*	0.23 ± 0.06*	3.85 ± 1.97*	2.22 ± 1.33†
Spleen	Untreated Fabry mice	N/D	26.37 ± 5.47	29.57 ± 2.11	20.65 ± 4.39
	Wild-type mice	N/D	0.31 ± 0.06	0.59 ± 0.01	0.2 ± 0.13
	Treated Fabry mice	N/D	5.04 ± 2.03*	22.71 ± 5.13	12.82 ± 6.39†
Heart	Untreated Fabry mice	N/D	2.02 ± 1.30	3.18 ± 0.23	3.1 ± 0.44
	Wild-type mice	N/D	0.22 ± 0.20	0.07 ± 0.00	0.03 ± 0.01
	Treated Fabry mice	N/D	0.69 ± 0.25†	1.50 ± 0.50*	1.70 ± 0.97†
Kidney	Untreated Fabry mice	13.26 ± 0.95	13.69 ± 1.00	16.1 ± 1.16	12.48 ± 2.96
	Wild-type mice	1.39 ± 0.10	1.60 ± 0.11	1.37 ± 0.28	0.96 ± 0.81
	Treated Fabry mice	9.83 ± 1.12†	12.65 ± 3.57	13.85 ± 2.94	16.56 ± 9.12
Lung	Untreated Fabry mice	3.57 ± 0.48	6.04 ± 1.99	7.22 ± 2.31	7.46 ± 1.70
	Wild-type mice	0.27 ± 0.06	0.23 ± 0.04	0.38 ± 0.13	0.56 ± 0.07
	Treated Fabry mice	2.04 ± 0.19*	1.38 ± 0.68*	5.61 ± 1.36	6.45 ± 3.21

Gb3 levels are expressed as average ± SD. N/D, not determined.
*, $P < 0.01$; †, $P < 0.05$ vs. untreated Fabry mice.

the increased AGA activity until week-five postinfection, suggesting an uptake of the secreted recombinant enzyme that would account for part of the α-gal A activity seen in these tissues. This observation is further supported by near-normal levels of Gb3 in organs in addition to liver at the 2-week time point. The possibility of the enzyme reuptake secreted from the liver must be considered. Possibly, the secreted enzyme interacts with mannose-6-phosphate and/or mannose receptors and the enzyme is internalized and delivered to the cells that contain stored Gb3.

We see a progressive decline (50%) of the AGA activity in liver at 5 and 15 weeks, leaving the residual enzyme activity at 5.5% ± 1% of normal activity at 15 weeks. However, these enzyme levels appear to be sufficient to maintain a 40–60%

correction of the Gb3 levels in liver and other organs. Transduced liver tissue sections showed minimal or no staining with the Gb3-monoclonal antibody in contrast to the untreated mouse liver at 15 weeks. It is not clear why we see an increase in the AGA enzyme levels at 25 weeks compared to 15 weeks posttransduction. One should not rule out the possibility that an integrated rAAV-AGA could account for some of the additional AGA activity seen. Using portal vein administration of rAAV vectors, Nakai *et al.* (16) observed that single-stranded rAAV genomes become double-stranded, circularized, and concomitant with a slow rise, eventually reach steady-state levels of transgene expression. Over time, some of the stabilized genome
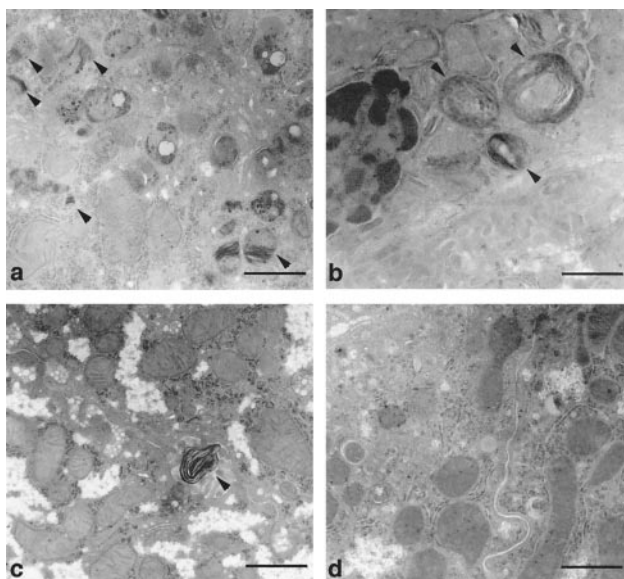
Fig. 5. Electron microscopy analysis of Fabry liver with and without rAAV-AGA treatment. Distinct lipid inclusions (arrows) are seen in hepatocytes (*a*) and Kupffer cells (*b*) in the nontransduced Fabry livers. Hepatocytes (*c*) and Kupffer cells (*d*) at 5 weeks posttreatment. An occasional inclusion body seen in same representative liver sample (*c*). [Bar = 1 μm.]
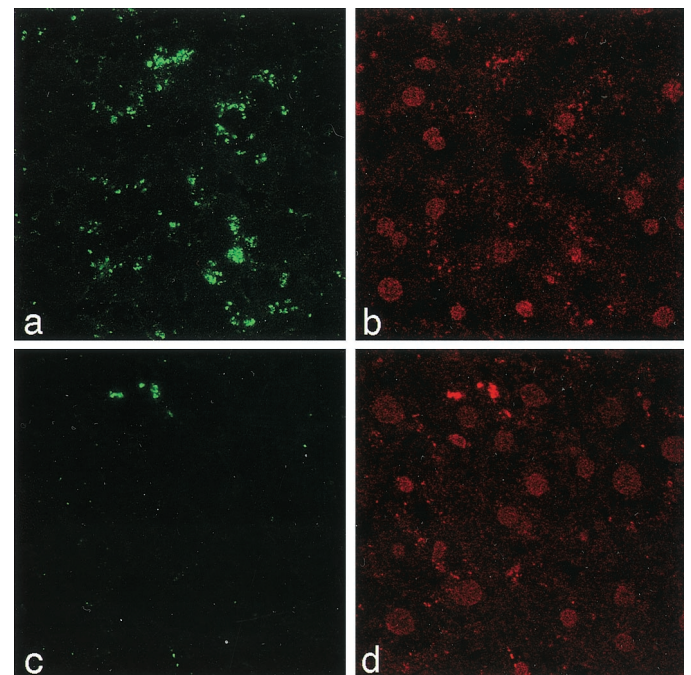
Fig. 6. Immunofluorescent staining of livers with FITC-conjugated anti-Gb3 monoclonal antibody. Age-matched Fabry mouse that was not transduced with rAAV-AGA (*a*). Fabry mouse at 15 weeks posttreatment (*c*). The nuclei were counterstained with propidium iodide (*b* and *d*).

Jung *et al.*

becomes integrated into the mouse chromosomal DNA. Conversely, a progressive decline of the AGA levels in liver and the reelevation of Gb3 levels could suggest an anti-AGA immune response. One would expect the AGA null mice to develop an immune response because the mice are naïve to the recombinant human α-gal A. However, the low AGA-specific response that belonged to a single subclass (IgG1) failed to substantiate the development of neutralization antibodies to the recombinant AGA. More recently, Xiao et al. (41) showed that delivery of a transgene into the portal circulation would elicit a T-cell-independent antibody response that was short-lived in comparison to a T-cell-dependent response.

In conclusion, we have demonstrated that a single hepatic portal vein administration of a rAAV-AGA can result in persistent expression and long-term phenotypic correction in the murine model of Fabry disease. The strategy of vector delivery into a depot organ, such as liver, may be useful for a number of lysosomal disorders. Moreover, the lack of toxicity and a consistent immune response renders this approach as a pragmatic choice for Fabry gene therapy.

1. Brady, R. O., Gal, A. E., Bradley, R. M., Martensson, E., Warshaw, A. L. & Laster, L. (1967) *N. Engl. J. Med.* **276,** 1163–1167.
2. Bishop, D. F., Calhoun, D. H., Bernstein, H. S., Hantzopoulos, P., Quinn, M. & Desnick, R. J. (1986) *Proc. Natl. Acad. Sci. USA* **83,** 4859–4863.
3. Bishop, D. F., Kornreich, R. & Desnick, R. J. (1988) *Proc. Natl. Acad. Sci. USA* **85,** 3903–3907.
4. Ohshima, T., Murray, G. J., Nagle, J. W., Quirk, J. M., Kraus, M. H., Barton, N. W., Brady, R. O. & Kulkarni, A. B. (1995) *Gene* **166,** 277–280.
5. Ohshima, T., Murray, G. J., Swaim, W. D., Longenecker, G., Quirk, J. M., Cardarelli, C. O., Sugimoto, Y., Pastan, I., Gottesman, M. M., Brady, R. O. & Kulkarni, A. B. (1997) *Proc. Natl. Acad. Sci. USA* **94,** 2540–2544.
6. Von Figura, K. & Hasilik, A. (1986) *Annu. Rev. Biochem.* **55,** 167–193.
7. Dahms, N. M., Lobel, P. & Kornfeld, S. (1989) *J. Biol. Chem.* **264,** 12115–12118.
8. Brady, R. O., Tallman, J. F., Johnson, W. G., Gal, A. E., Leahy, W. R., Quirk, J. M. & Dekaban, A. S. (1973) *N. Engl. J. Med.* **289,** 9–14.
9. Neufeld, E. F. (1991) *Annu. Rev. Biochem.* **60,** 257–280.
10. Schiffmann, R., Murray, G. J., Treco, D., Daniel, P., Sellos-Moura, M., Myers, M., Quirk, J. M., Zirzow, G. C., Borowski, M., Loveday, K., et al. (2000) *Proc. Natl. Acad. Sci. USA* **97,** 365–370.
11. Sugimoto, Y., Aksentijevich, I., Murray, G. J., Brady, R. O., Pastan, I. & Gottesman, M. M. (1995) *Hum. Gene Ther.* **6,** 905–915.
12. Takenaka, T., Qin, G., Brady, R. O. & Medin, J. A. (1999) *Hum. Gene Ther.* **10,** 1931–1939.
13. Takenaka, T., Murray, G. J., Qin, G., Quirk, J. M., Ohshima, T., Qasba, P., Clark, K., Kulkarni, A. B., Brady, R. O. & Medin, J. A. (2000) *Proc. Natl. Acad. Sci. USA* **97,** 7515–7520. (First Published June 6, 2000; 10.1073/pnas.120177997)
14. Ohshima, T., Schiffmann, R., Murray, G. J., Kopp, J., Quirk, J. M., Stahl, S., Chan, C. C., Zerfas, P., Tao-Cheng, J. H., Ward, J. M., et al. (1999) *Proc. Natl. Acad. Sci. USA* **96,** 6423–6427.
15. Ziegler, R. J., Yew, N. S., Li, C., Cherry, M., Berthelette, P., Romanczuk, H., Ioannou, Y. A., Zeidner, K. M., Desnick, R. J. & Cheng, S. H. (1999) *Hum. Gene Ther.* **10,** 1667–1682.
16. Nakai, H., Storm, T. A. & Kay, M. A. (2000) *J. Virol.* **74,** 9451–9463.
17. Wang, B., Li, J. & Xiao, X. (2000) *Proc. Natl. Acad. Sci. USA* **97,** 13714–13719. (First Published November 28, 2000; 10.1073/pnas.240335297)
18. During, M. J., Symes, C. W., Lawlor, P. A., Lin, J., Dunning, J., Fitzsimons, H. L., Poulsen, D., Leone, P., Xu, R., Dicker, B. L., et al. (2000) *Science* **287,** 1453–1460.
19. Samulski, R. J., Chang, L.-S. & Shenk, T. (1989) *J. Virol.* **63,** 3822–3828.
20. Graham, F. L., Smiley, J., Russell, W. C. & Nairn, R. (1977) *J. Gen. Virol.* 3 **6,** 59–74.
21. Kusiak, J. W., Quirk, J. M. & Brady, R. O. (1978) *J. Biol. Chem.* **253,** 184–190.
22. Towbin, H., Staehelin, T. & Gordon, J. (1979) *Proc. Natl. Acad. Sci. USA* **76,** 4350–4354.
23. Rose, G. R. & Oklander, M. (1965) *J. Lipid Res.* **6,** 428–431.
24. Ullman, M. D. & McClure, R. H. (1977) *J. Lipid Res.* **8,** 371–378.
25. Ito, K., Kotani, M., Tai, T., Suzuki, H., Utsunomiya, T., Inoue, H., Yamada, H., Sakuraba, H. & Suzuki, Y. (1993) *Clin. Genet.* **44,** 302–306.
26. Liang, H., Narum, D. L., Fuhrmann, S. R., Luu, T. & Sim, B. K. (2000) *Infect. Immun.* **68,** 3564–3568.
27. Wolfe, J. H., Sands, M. S., Barker, J. E., Gwynn, B., Rowe, L. B., Vogler, C. A. & Birkenmeier, E. H. (1992) *Nature (London)* **360,** 749–753.
28. Desnick, R. J., Ioannou, Y. A. & Eng, C. M. (1996) in *The Metabolic and Molecular Bases of Inherited Disease*, eds. Scriver, C. R., Beaudet, A. L., Sly, W. S. & Valle, D. (McGraw-Hill, New York), pp. 2741–2784.
29. Xiao, X., Li, J. & Samulski, R. J. (1996) *J. Virol.* **70,** 8098–8108.
30. Kessler, P. D., Podsakoff, G. M., Chen, X., McQuiston, S. A., Colosi, P. C., Matelis, L. A., Kurtzman, G. J. & Byrne, B. J. (1996) *Proc. Natl. Acad. Sci. USA* **93,** 14082–14087.
31. Vance, D. E., Krivit, W. & Sweeley, C. C. (1969) *J. Lipid Res.* **10,** 188–192.
32. Hozumi, I., Nishizawa, M., Ariga, T. & Miyatake, T. (1990) *J. Lipid Res.* **31,** 335–340.
33. Elleder, M. (1985) *Acta Histochem.* **77,** 33–36.
34. Futagawa, Y., Pkamoto, T., Ohashi, T. & Eto, Y. (2000) *Res. Exp. Med. (Berl.)* **99,** 263–274.
35. Nakai, H., Herzog, R. W., Hagstrom, J. N., Walter, J., Kung, S. H., Yang, E. Y., Tai, S. J., Iwaki, Y., Kurtzman, G. J., Fisher, K. J., et al. (1998) *Blood* **91,** 4600–4607.
36. Ohashi, T., Watabe, K., Uehara, K., Sly, W. S., Vogler, C. & Eto, Y. (1997) *Proc. Natl. Acad. Sci. USA* **94,** 1287–1292.
37. Schiffmann, R., Kopp, J. B., Austin, H., Moore, D. F., Sabnis, S., Weibel, T., Balow, J. E. & Brady, R. O. (2000) *Am. J. Hum. Genet.* **67,** Suppl. 2, 38.
38. Wang, L., Nichols, T. C., Read, M. S., Bellinger, D. A. & Verma, I. M. (2000) *Mol. Ther.* **1,** 154–158.
39. Lee, H. C., Kim, S. J., Kim, K. S., Shin, H. C. & Yoon, J. W. (2000) *Nature (London)* **408,** 483–488.
40. Abe, A., Gregory, S., Lee, L., Killen, P. D., Brady, R. O., Kulkarni, A. & Shayman, J. A. (2000) *J. Clin. Invest.* **105,** 1563–1571.
41. Xiao, W., Chirmule, N., Schnell, M. A., Tazelaar, J., Hughes, J. V. & Wilson, J. M. (2000) *Mol. Ther.* **1,** 323–329.

MEDICAL SCIENCES